Crack-Free 3D Hybrid Microstructures from Photosensitive Organosilicates as Versatile Photonic Templates

Yongan Xu, Xuelian Zhu, and Shu Yang*

Department of Materials Science and Engineering, University of Pennsylvania, 3231 Walnut Street, Philadelphia, Pennsylvania 19104

ABSTRACT We fabricated diamond-like microstructures from epoxy-functionalized cyclohexyl polyhedral oligomeric silsesquioxanes (POSS) through four-beam interference lithography. The 3D structure was maintained when calcined at a temperature up to 1100 °C, and crack-free samples over a large area (~5 mm in diameter) were obtained when the POSS films were heated at 500 °C under an Ar environment or treated with a low intensity oxygen plasma. In the latter, the volume fraction of the 3D porous structures could be fine-tuned by plasma etching time and power. Both Fourier transform infrared (FT-IR) spectroscopy and energy-dispersive X-ray (EDX) spectroscopy analysis suggested that the presence of carbon materials in the films enhanced the crack resistance of 3D POSS structures treated under Ar or oxygen plasma. Since POSS and its derivatives could be easily removed by HF solution at room temperature, we demonstrated high fidelity replication of the 3D porous structures to biocompatible poly(glycidyl methacrylate) (PGMA) and elastomeric poly(dimethylsiloxane) (PDMS). Importantly, the whole fabrication process (template fabrication, infiltration, and removal) was carried out at room temperature. Finally, we illustrated the application of 3D PDMS film as a reversible and repeatable color-changing, flexible photonic crystal.

KEYWORDS: multibeam interference lithography · photonic crystal · high fidelity · crack-free · thermal and mechanical stability · templating · POSS · PDMS · hydrogels

Three-dimensional (3D) structures with (sub)micrometer periodicity are of interest for a wide range of applications, including photonic[1] and phononic crystals,[2,3] optical data storage,[4] microfluidics,[5,6] optofluidics,[7] sensors,[8−10] tissue scaffolds,[11] as well as controlled delivery.[12] Various fabrication methods, including self-assembly, standard layer-by-layer microfabrication process, and nonconventional optical lithography, have been studied to create various 3D structures with (sub)micrometer periodicity in a controlled manner.[13−15] Among them, laser-based microfabrication techniques, such as multibeam interference lithography, offer efficient routes to fabricate 2D and 3D complex structures with periods of 0.3 to 6 μm over large area with controlled defects. The requirement of photosensitive materials, however, limits direct fabrication of 3D microstructures over a wide range of materials that are not compatible with a lithographic process, such as high index semiconductors for complete photonic band gap (PBG) properties, and responsive hydrogels and elastomers for dynamic tuning of the structure−property.

Alternatively, the patterned 3D polymer structures can be used as templates for backfilling with organic, hybrid, and inorganic materials, followed by removal of the polymer template to obtain inverse 3D structures. Because the 3D templates fabricated by interference lithography are bicontinuous networks, after backfilling, they have to be removed either by decomposition or by dissolution. In interference lithography, negative-tone photoresists (*e.g.*, SU-8) are commonly used,[13,15] which form highly cross-linked 3D networks that are difficult to remove by solvent or heat below 400 °C. Therefore, it is not possible to template other organic polymers, specifically, responsive hydrogels and elastomeric poly(dimethylsiloxane) (PDMS) films, from the negative-tone resist templates. A handful of groups have used commercially available positive-tone resist, AZ5214 (Clariant International Ltd.) to create 2D and 3D structures,[3,13] which can be easily dissolved in an organic solvent after infiltration. Jang *et al.* fabricated a 3D PDMS film from the corresponding AZ5214 template as a tunable phononic crystal.[3] However, the aromatic groups in AZ series resists are highly absorbing in the UV−vis region, thus limiting the film thickness of 3D structures to less than 5 μm.[3]

Additionally, a high deposition temperature (>400 °C) is necessary when templating high refractive index (*e.g.*, Si and TiO_2) photonic crystals, at which the polymer templates begin to decompose. Therefore, a double templating process *via* silica replica of the polymer template has often been

*Address correspondence to shuyang@seas.upenn.edu.

Received for review July 10, 2009 and accepted September 16, 2009.

Published online September 22, 2009.
10.1021/nn9007803 CCC: $40.75

employed.[16,17] Backfilling and calcination processes (both >400 °C), however, often suffer from large volume shrinkage that causes pattern collapse and crack formation.[18−20] Overall, the fidelity of the final 3D structure is critically dependent on that of the template and its backfilling and removal processes.

An ideal 3D template should be (1) compatible with photolithographic process, (2) thermally and mechanically robust above 400 °C, and (3) easy to remove at room temperature by either dry etching or dissolution. Polyhedral oligomeric silsesquioxanes (POSS) are a unique class of hybrid materials, which possess the structure of cube-octameric frameworks with eight organic corner groups. They have a chemical composition of $RSiO_{1.5}$ with thermal and mechanical properties intermediate between SiO_2 and organic polymers. The functional groups, such as epoxy and (meth)acrylate, can be introduced to make the POSS materials photopatternable.[21−25] Further, the presence of organic moieties makes POSS compatible with various polymer systems, as well as enhance crack resistance of the film.[26]

Recently, we have investigated the direct fabrication of 3D silica-like structures from epoxy-functionalized cyclohexyl polyhedral oligomeric silsesquioxanes (epoxy POSS) using four-beam interference lithography.[25] We showed that the 3D epoxy POSS structures were maintained without global volume shrinkage during the heat treatment (up to 400 °C) by thinning the struts that connect motifs. Since organosilicates can be conveniently converted to silica by thermal decomposition of the organic moieties, which can be subsequently removed by aqueous hydrofluoric acid (HF) solution at room temperature, the 3D POSS structures are attractive as templates for infiltration of a wide range of organic and inorganic materials. However, we found microcracks had appeared all over the POSS film when heating above 400 °C in air due to the residue strain in the porous film caused by the large mass loss and materials shrinkage. To eliminate the cracks and maintain the high fidelity of the 3D structures, a few groups have investigated application of a sacrificial layer between the film and substrate,[19,27] such that the obtained free-standing films shrink isotropically during sintering to minimize residual strain within the film. Nevertheless, this approach is not ideal for fabrication of on-chip devices. Recently, Orilall *et al.*[28] have shown stable macroporous 3D structures from polystyrene colloidal templates, which were heated under inert atmosphere up to 900 °C. The stability was attributed to the formation of amorphous/graphitic-like carbon within the template.

Here, we demonstrate the fabrication of crack-free 3D silica-like structures over a large area (~5 mm in diameter) when treating the diamond-like epoxy POSS films in two different processes, including thermal treatment under an Ar environment and O_2 plasma etching. The diamond-like POSS films were fabricated through four-beam interference lithography, followed by calcination under either an O_2 or Ar environment or O_2 plasma etching, to investigate the thermal and mechanical stability of the resulting films. The 3D structure was maintained when calcined at a temperature up to 1100 °C, and crack-free samples were obtained when the POSS films were treated with a low intensity O_2 plasma or heated at 500 °C under an Ar environment, in contrast to crack formation when heated in O_2. Fourier transform infrared (FT-IR) spectroscopy and energy-dispersive X-ray (EDX) spectroscopy analysis suggested that the chemical nature and composition of the films remained the same as POSS after O_2 plasma, whereas a large quantity of amorphous carbon was found in the film calcined in Ar, which might contribute to the crack resistance of the films. In contrast, the POSS film was nearly completely converted to silica when calcined in O_2. Further, the volume fraction of the porous film could be conveniently controlled by O_2 plasma etching time and power. Since the epoxy POSS film and its derivatives could be easily removed by HF solution at room temperature, we demonstrated high fidelity replication of the 3D porous structures to biocompatible poly(glycidyl methacrylate) (PGMA) and elastomeric PDMS. We note that the whole fabrication process (template fabrication, infiltration, and removal) was carried out at room temperature. Finally, we illustrated one potential application of 3D PDMS film as a reversibly color-changing, flexible photonic crystal.

RESULTS AND DISCUSSION

The 3D POSS structures were fabricated by four-beam interference lithography of the negative-tone resist, epoxycyclohexyl POSS (Scheme 1).[20] Compared to SU-8 materials, where 2 wt % photoacid generators (PAG) were used, 1 wt % or less PAG was sufficient for the POSS photoresist, and the exposure time was half of that for SU-8 under the same exposure power. This can be attributed to the lower glass

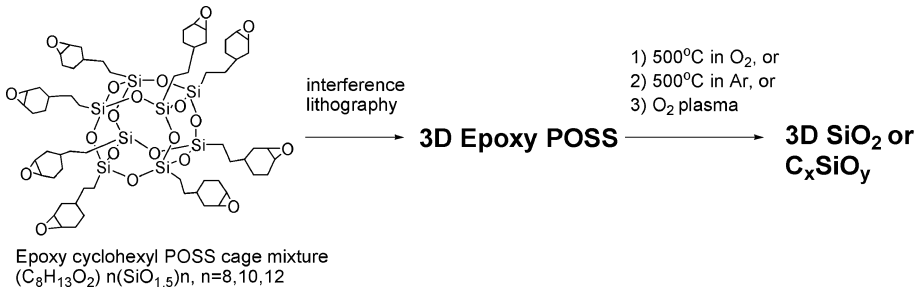

Scheme 1. Schematic illustration of epoxycyclohexyl-functionalized POSS cage structure and its conversion to silica-like structures under different conditions.

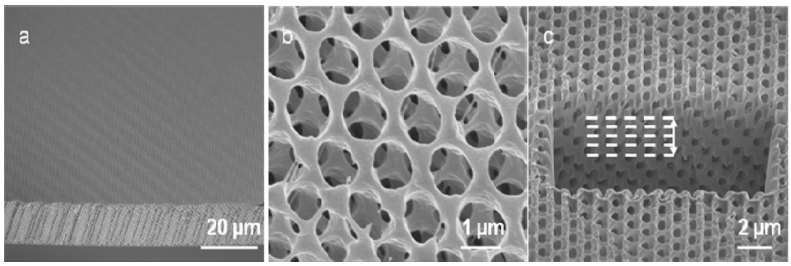

Figure 1. SEM images of 3D POSS. (a) Large view. (b) Top view. (c) Cross-sectional view. The sample was focus-ion-milled and tilted at 45°.

TABLE 1. Characteristics of Diamond-like POSS Structure Fabricated by Holographic Lithography

	POSS (n = 1.52)	
materials	pitch in the (111) plane	distance between the adjacent lattice planes in the [111] direction
experimental (μm)	0.98	0.68
calculated (μm)	0.98	1.30
shrinkage (%)	0	48
volume shrinkage (%)	48	

transition temperature (T_g) of epoxy POSS (~3 °C by differential scanning calorimetry, DSC) than that of SU-8 (50 °C). Therefore, the acid diffusion was much faster in epoxy POSS, resulting in a lower insolubility threshold. The resulting 3D structures were characterized by scanning electron microscopy (SEM). It is known that negative-tone photoresists have relatively large film shrinkage during photo-cross-linking and developing steps when films become more densified.[29,30] Quantification of the shrinkage of the fabricated 3D POSS structures will be important to estimate the residual strain imposed in the film for later processing and to predict the influence to the structural, mechanical, and optical properties. First, we reconstructed the 3D structures based on SEM images obtained at different crystal planes (Figure 1) and compared the lattice constants to the calculated values. The detailed calculation and reconstruction of the theoretical 3D structures were reported earlier.[29] A refractive index of 1.52 was used for epoxy POSS in our calculation, which was determined by ellipsometry measurement. As seen in Table 1, there is 48% shrinkage in the [111] direction but no shrinkage in the (111) plane, leaving large residual strain within the POSS film. The difference in shrinkage in different directions can be explained by the substrate confinement effect, where the porous structure can shrink freely in the vertical direction but is restricted in the horizontal plane.[29,31] The slightly larger shrinkage of 3D POSS in the [111] direction in comparison to SU-8 (41%)[29] may be due to the lower molecular weight of the epoxy POSS precursor (with lower T_g), resulting in larger density change after photo-cross-linking.

Previously, we have studied the thermal and mechanical stability of the 3D epoxy POSS when sintered at 500 °C in air to remove the organic contents (Scheme 1).[25] The 3D structure was found thermally stable up to 500 °C in air or O_2, and the POSS film was converted to silica. However, microcracks appeared throughout the film (Figure 2) due to large mass loss and mismatch of coefficient of thermal expansion (CTE) between the porous silica structure and the glass substrate. While the crack-free area could be found in local domains (~100 × 100 μm^2), the formation of microcracks over a mm^2 area remains undesirable for templating high index materials, which often requires high deposition temperature (400−800 °C). In turn, it will decrease the quality of the film for potential photonic device application.

Orilall *et al.* recently have shown that heating the polystyrene colloidal templates under an inert atmosphere up to 900 °C converts the polymer into sturdy amorphous/graphitic-like carbon, which prevents the collapse of the macroporous structures.[28] To investigate whether this mechanism was applicable to our system, we performed thermal treatment under Ar atmosphere at a temperature varied from 500 to 1100 °C for 1 h. We found that the whole film was crack-free at 500 °C in Ar in contrast to that heated in O_2 (see Figure 3), whereas cracks appeared at 1100 °C, probably due to large thermal coefficient mismatch between the film and the substrate. Here, the film was transferred from a cover glass to a Si wafer since glass became softened above 1000 °C. Compared to the original POSS structure, the pore size became bigger after calcination (Figure 3c) due to the large mass loss. Further, the optical

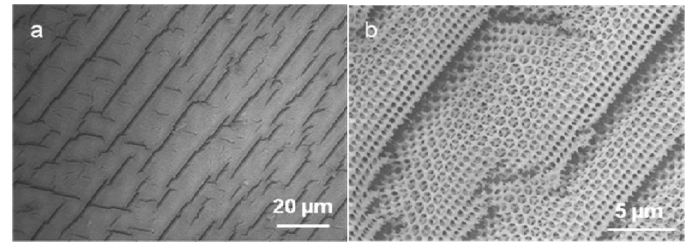

Figure 2. SEM images of 3D POSS structures after calcination at 500 °C for 1 h in O_2. (a) Large view. (b) Close-up view.

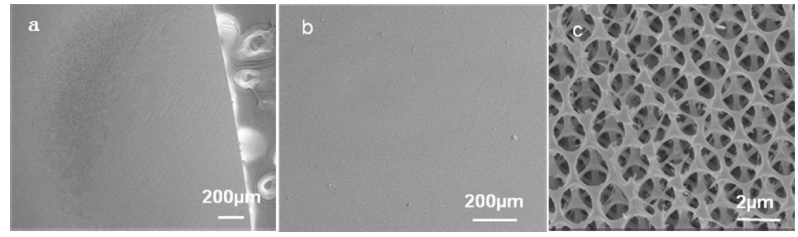

Figure 3. SEM images of 3D POSS structures after calcination at 500 °C for 1 h under an Ar environment at different magnifications: (a) 150×, (b) 500×, and (c) 50 000×.

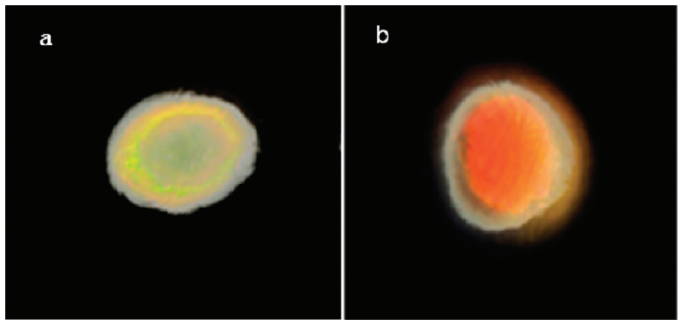

Figure 4. Optical images of 3D POSS films (a) before and (b) after heating at 500 °C for 1 h in Ar. The images were taken at the same light illumination angle of 45°.

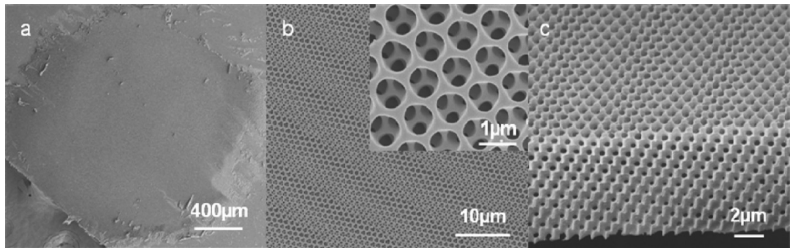

Figure 5. SEM images of 3D POSS structures after O_2 plasma etching (power of 30 W) for 1 h. (a) Large view. (b) Top view. Inset: close-up view. (d) Cross-sectional view.

photograph of the 3D POSS structure after thermal treatment in Ar (Figure 4b) appeared darker compared to that of the as-fabricated one (Figure 4a), which might be due to the formation of carbon in the film. Surprisingly, no major microcracks were observed under optical microscope, which was further manifested by SEM images under different magnifications (Figure 3).

In addition to the film quality, the filling volume fraction of the template, thus, the porosity of the inversed photonic crystal, plays an important role to open a complete band gap.[17] Thus, we attempted a second approach, that is, a dry etching method using O_2 plasma, to remove the organic moieties at room temperature (Scheme 1). Compared to thermal treatment, the latter approach will offer the flexibility to control the filling volume fraction. As seen in Figure 5, when the film was exposed to a low power (30 W) O_2 plasma for 1 h, a crack-free film over ~5 mm in diameter was obtained, whereas the skeleton of the 3D structure apparently became thinner (strut width, ~130 nm) (Figure 5b) in comparison to that of the original POSS film (~283 nm) (Figure 1b). If the film remained in the plasma chamber continuously for a few hours, it became rather hot and microcracks were observed as those seen in the samples calcined in O_2 (see Figure 2). If the sample was taken out of the plasma chamber intermittently for cooling, then etched again, for example, for another 2 h and 40 min, the film remained crack-free, while the porosity was increased to 70% and the skeleton was as thin as ~78 nm (Figure 6a,b). When the total plasma time was increased to 5 h 40 min, the top surface of the porous structure began to collapse (Figure 6c) and the 3D structure was completely destroyed after O_2 plasma treatment for a total of 10 h (Figure 6d). Since the plasma etching is a top-down process, we have been curious about how uniform the etching was throughout the film. Surprisingly, in contrast to the result shown in Figure 6c with long etching time, at a relatively shorter etching time (<4 h), the porosity and skeleton thickness were rather uniform throughout the film in the 3D structures according to the cross-sectional SEM images (Figures 5c and 6b). We think both the low etching intensity in our plasma chamber and relatively thin film of 3D structures (<10 μm thick) may contribute to the rather uniform etching results. Nevertheless, the experiments demonstrated that we could vary the film porosity up to 80% before the 3D structure collapsed simply by changing the O_2 plasma treatment time, which would allow us to manipulate the photonic band gap properties.

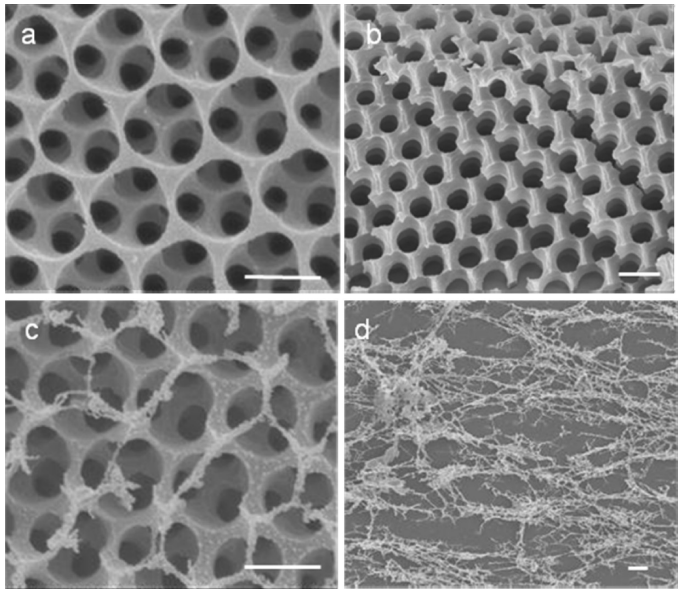

Figure 6. SEM images of 3D POSS structures after O_2 plasma etching at different time: (a,b) 3 h 40 min, (c) 5 h 40 min, and (d) 10 h in total. The films were continuously etched for 1−2 h before taken out and cooled and put back to the chamber for etching. Scale bar = 1 μm.

To understand the underlying mechanism of the high fidelity 3D structures obtained after thermal treatment in either Ar or O_2 plasma, we investigated the chemical nature of the films in different processes using FT-IR and EDX spectroscopy analysis. As seen in Figure 7, we have identified 10 IR bands: A (3000−3700 cm^{-1}), B (2800 −3000 cm^{-1}), C (1636 cm^{-1}), D (1350−1450 cm^{-1}), E (1245 cm^{-1}), F (1000−1150 cm^{-1}), G (1076 cm^{-1}), H (955 cm^{-1}), I (870−890 cm^{-1}), J (780−800 cm^{-1}). Some of the Si−O peaks and C−O ether or epoxy ring peaks overlap. The detailed assignment of the observed IR peaks is summarized in Table 2.

In comparison to the IR spectrum of SiO_2 as a reference,[32] it is clear that all films contain a certain amount of carbon. Heating the film in O_2 removed most carbon,

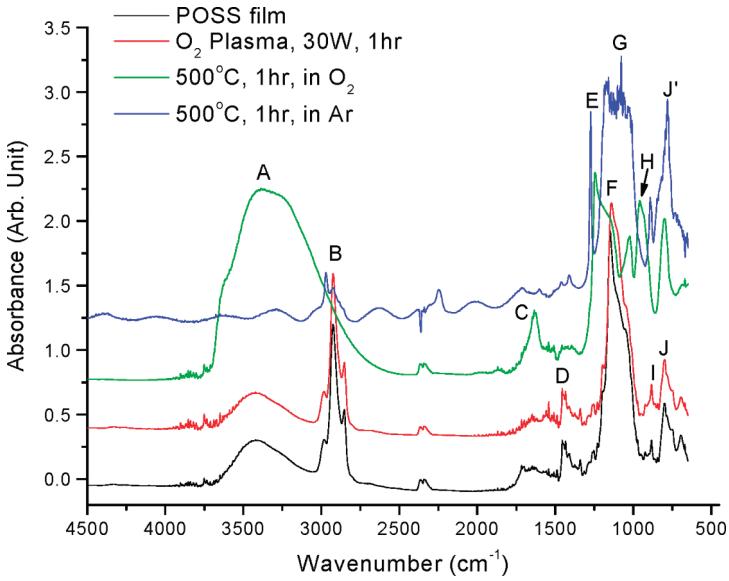

Figure 7. FT-IR spectra of 3D POSS structures treated under different conditions.

as evidenced with the disappearance of C−H stretch peak (B, 2970 cm^{-1}), and the film possessed a large quantity of Si−OH (see peaks A and H). The appearance of carbonyl peak C is probably due to the oxidation of the film. For the films heated at 500 °C in Ar, a large amount of CH_2 groups (see peaks B and D) was removed but no −OH groups were formed, in contrast to the film treated in O_2. The intensity of shoulder G (O−Si−O long chain) increased from the original POSS to O_2 plasma treated one and became a rather broad peak in film treated in Ar, indicating that the cage structures with O−Si−O short chains may have been collapsed into ladder or random structures.[32,33] The appearance of E and shift of J (800 cm^{-1}) to J′ (780 cm^{-1}) with increased intensity, both from Si−C stretch, further confirms the presence of carbon in the film treated in Ar.[34] The POSS film after O_2 plasma treatment for 1 h was nearly identical to that of the original film.

To quantify the elemental composition of the 3D POSS films treated under different conditions, we performed EDX mapping analysis. The film was transferred to an Al substrate before EDX mapping to eliminate substrate contribution of Si or O. As seen in Table 3, for a POSS film treated in Ar at 500 °C for 1 h, the O/Si ratio was close to 2. However, a significant amount of residual carbon, 28.83 wt %, remained in the film, in contrast to a trace amount of carbon (1.67 wt %) in the POSS film heated in O_2. For the latter, the O/Si ratio was also close to 2, indicating nearly complete conversion of POSS to silica. For O_2 plasma treated (30 W, 1 h) film, the C/Si ratio was nearly identical to the original POSS film, in agreement with FT-IR results, with 56.31 wt % carbon remaining in the film. On the basis of stoichiometric calculation, the residual carbon from the heat treatment in Ar should exist as amorphous/graphitic-like material as suggested by Orilall *et al.*,[28] not silicon oxycarbide. Supporting this, the above treated templates could be easily removed by HF aqueous solution (see discussion in the next section), whereas the silicon oxycarbide film is known to be not soluble in HF aqueous solution.[35] In any case, both FT-IR and EDX analysis suggested that the presence of carbon materials in the films enhanced the crack resistance of 3D POSS structures.

Since both the POSS film and its derivatives can be readily dissolved in HF aqueous solution, they are attractive as robust and versatile templates for replication of a wide range of materials that can be processed either at low (*e.g.*, organics, polymers) or at high temperatures (*e.g.*, semiconductors). The application of 3D POSS templates for fabrication of high index semiconductor photonic crystals will be discussed elsewhere. Here, we demonstrated the utility of 3D POSS structures for room-temperature templating of functional 3D polymeric structures, including PGMA and PDMS. Both of them are biocompatible, and their 3D porous structures are of interest as a scaffold for tissue engineering.[36,37] Moreover, PDMS is elastomeric. Its low Young's modu-

TABLE 2. Observed IR Peaks and Their Assignments for Epoxy POSS Films Treated under Different Conditions

peak	POSS after cross-linking	POSS after O_2 plasma	POSS 500 °C, in O_2	POSS 500 °C, in Ar	SiO_2[a]	peak assignment
A	3000−3700	3000−3700	3000−3700			−OH stretch
B	2800−3000	2800−3000		2800−3000		$-CH_2$ stretch
C			1636			−C═O stretch
D	1350−1450	1350−1450				$-CH_2$ deformation
E			1245	1272		$-CH_3$ deformation
F	1150−1000	1150−1000	1150−1000	1150−1000		−C−O−C ether stretch
	1137	1137	1137	1137	1186	−O−Si−O− short chain vibration
G	1076	1076		1076	1087	−O−Si−O− long chain
H			955			−Si−OH stretch
I	878	878		887		epoxy ring C−O−C deformation
J, J′	800	790	800	780	810	Si−C stretch

[a]From ref 32.

TABLE 3. Elemental Analysis of 3D POSS Structures Treated under Different Conditions

	bare POSS film[a]	O_2 plasma treated		500 °C in O_2		500 °C in Ar	
element	relative weight (%)	relative weight (%)	relative atomic (%)	relative weight (%)	relative atomic (%)	relative weight (%)	relative atomic (%)
C	58.54	56.31	66.88	1.67	2.70	28.83	40.32
O	24.39	28.47	25.39	56.68	68.60	37.88	39.77
Si	17.07	15.22	7.73	41.64	28.71	33.29	19.91
total	100.0	100.00	100.00	100.00	100.00	100.00	100.00

[a]The composition was calculated based on chemical fomulation of epoxy POSS provided by Hybrid Plastics, $(C_8H_{13}O)_n(SiO_{1.5})_n$.

lus (1−3 MPa) makes it easily deformed under an external force or by exposure to an organic solvent. Recently, such deformation has been harnessed for tunable phononic crystals.[3]

Because epoxy POSS is highly transparent in the UV−vis region, we have successfully fabricated 3D POSS structures with film thickness up to 30 μm in comparison to <5 μm using AZ5214.[3] The inverse 3D PGMA and PDMS structures were obtained by first filling the viscous precursors into the porous POSS template, followed by photopolymerization (for PGMA) or thermal curing (for PDMS), and HF etching (Scheme 2). Since PDMS is more hydrophobic than the POSS template, in order to remove the POSS template, a little bit of organic solvent was added in the HF solution to achieve good wettability at the POSS/PDMS interface. This solvent must be soluble in water but should neither dissolve nor swell the PDMS film. Among many organic solvents, DMSO offers the ideal combination as the wetting solvent, which has a PDMS swelling ratio of 1.00.[38] In our experiments, no apparent swelling was observed after the PDMS sample was immersed in DMSO for approximately 2 h. In the case of PGMA replication, the HF aqueous solution has good wettability on PGMA, thus, no organic solvent was added. To estimate the POSS etching time, a control experiment was first conducted by immersing a bare 3D POSS film in the same HF solution, which was found completely dissolved in less than 10 min. For the PGMA or PDMS/POSS composites, ~50 min was necessary to remove the POSS template.

As seen in Figure 8, the PGMA and PDMS precursors were completely filled into the templates and faithfully replicate the 3D diamond-like structures. Because the whole fabrication process was achieved at room temperature, including fabrication of template, infiltration of precursors and polymerization, and removal of the template, high fidelity films that were completely crack-free over the entire sample area (~5 mm in diameter) were obtained. Compared to many reported templating processes using highly cross-linked negative-tone resist (*e.g.*, SU-8), which requires high decomposition temperature (≥400 °C in air) to remove the template, the POSS 3D structure is clearly advantageous and versatile for both high and low temperature templating. The fabrication procedure we demonstrated here can be straightforwardly applicable to many other materials, organic, hybrid, and ceramic materials, for fabrication of a wide range of 3D structures.

Finally, we illustrate the application of 3D PDMS film for flexible photonic switching. Since PDMS film is deformable in organic solvent[39] and/or under mechanical stretching,[40] 3D PDMS structures have been of interest as tunable photonic paper and inks[41] and phononic crystals.[3] Compared to solvent swelling-induced deformation, the use of mechanical force allows us to independently control the amount, direction (uniaxial or biaxial in planar directions or in vertical direction), and timing of strain applied to the PDMS film. This added controllability offers us flexibility to maneuver the porosity and lattice constant of the 3D structure, thus, optical properties *in real time*. As seen in Figure 9, when the photonic film was stretched uniaxially in-plane, the hue of crystal color gradually changed from bright yellow to red to dark green when the applied strain was increased from 0 to 22.6% (Figure 9b1−b8). When the strain was released, the color was completely recovered (Figure 9c1−c7; movie also available in Supporting Information). The wavelength of the structure color, λ, can be expressed by Bragg's

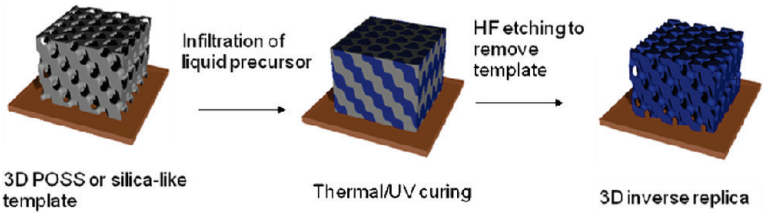

Scheme 2. Schematic illustration of the fabrication of 3D polymer structures templated from 3D POSS at room temperature.

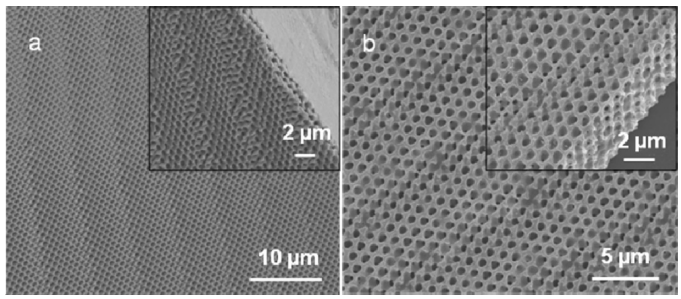

Figure 8. SEM images of 3D (a) PGMA and (b) PDMS structures after removal of the POSS template by HF etching. Insets: cross-sectional views.

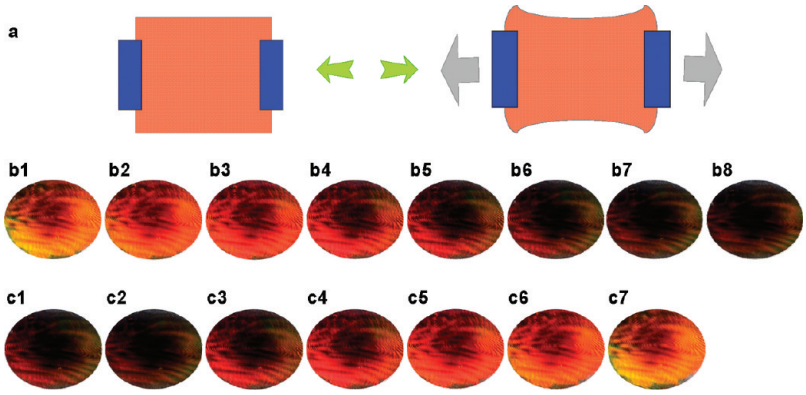

Figure 9. Reversibly in-plane stretching 3D PDMS structures. (a) Schematics of stretching. (b,c) Optical images of 3D PDMS after reversibly stretching (b) and releasing (c) the strain at different levels. The color changed gradually as the strain was increased or decreased. (b1,c7) 0%, (b2,c6) 3.2%, (b3,c5) 6.5%, (b4,c4) 9.7%, (b5,c3) 12.9%, (b6,c2) 16.1%, (b7,c1) 19.4%, and (b8) 22.6%.

equation with Snell's Law: $\lambda = 2d\sqrt{(n_e^2 - \sin^2\theta)}$, where d is the interplanar spacing of the planes, n_e is the effective refractive index, and θ is the angle of incident light. When stretched in the (111) plane, lattice constants increased along the stretching direction while that decreased in the perpendicular direction due to Poisson's ratio of PDMS ($\nu = 0.5$). These lattice-constant changes shift the optical path of the diffraction light accordingly, which in turn caused change of the diffraction color. Moreover, this color tuning of the PDMS sheet is reversible and repeatable. Detailed characterization of the stretched films and their manipulation will be reported elsewhere.

CONCLUSIONS

We fabricated diamond-like POSS structures through four-beam interference lithography and studied their thermal and mechanical stability either under thermal treatment or by O_2 plasma. The 3D structure was maintained when calcined at a temperature up to 1100 °C, and crack-free samples over a large area (~5 mm in diameter) were obtained when the POSS films were treated with a low intensity oxygen plasma or heated at 500 °C under an Ar environment, in contrast to crack formation when thermally treated in O_2. FT-IR and EDX spectra analysis suggested there was a large quantity of residual carbon left in the crack-free samples to enhance the crack resistance of the 3D structures. Further, we could fine-tune the filling volume fraction of the 3D POSS structures by varying the O_2 plasma treatment time and power. Since POSS and its derivatives could be easily removed by HF aqueous solution at room temperature, we demonstrated the utility of the 3D POSS structures as templates for high fidelity replication of the 3D porous structures into functional polymers, including PGMA and PDMS. Notably, the whole process (template fabrication, infiltration, and removal) was achieved at room temperature. Finally, we illustrated the application of 3D PDMS film as a reversible and repeatable color-changing, flexible photonic crystal. We believe that the organosilicate structure demonstrated here offers a thermally and mechanically robust yet versatile template for replication of a wide range of materials at both low and ultrahigh processing temperatures. The presented high fidelity templating and tuning of the optical properties of the replicated 3D PDMS films will provide important insights to create novel materials that are potentially useful for a wide variety of technological applications.

EXPERIMENTAL METHODS

Fabrication of 3D POSS Structures. The 3D POSS structure was fabricated by four-beam interference lithography following the procedure reported previously[20] using a visible diode-pumped Nd:YVO4 laser ($\lambda = 532$ nm). The photoresist solution (~80 wt %) was formulated by mixing epoxycyclohexyl POSS cage mixture (EP0408, Hybrid Plastics) and 1.0 wt % Irgacure 261 (Ciba Specialty Chemicals) as visible photoinitiator in propylene glycol monomethyl ether acetate (PGMEA, Aldrich). The film (thickness ~8 μm) was obtained by spin coating the photoresist solution on an O_2 plasma (PDC-001, Harrick Scientific Products, Inc.) cleaned glass at 2000 rpm for 30 s. Since the glass transition temperature of the epoxy POSS precursor is rather low, ~3 °C by DSC at a heating rate of 10 °C/min, the film was prebaked at 50 °C for about 40 min and 95 °C for 2 min to remove the solvent. After exposure to four-interfering beams (power of beam source ~ 0.7 w) for ~1 s, the film was post-exposure-baked at 50 °C for about 30 s and developed in PGMEA to remove unexposed or weakly exposed films, resulting in 3D microporous structures. To prevent the pattern collapse of the 3D film due to the capillary force upon drying in air, we dried the film using supercritical CO_2 dryer (SAMDRI-PVT-3D, tousimis) after the pattern development.

Post-Treatment of 3D POSS Structures. The fabricated 3D POSS films were post-treated by O_2 plasma etching and calcination in both O_2 and Ar environment, respectively. The O_2 plasma etching was performed in an O_2 plasma cleaner (PDC-001, Harrick Scientific Products, Inc.) at different time to achieve various filling volume fractions. The typical working power and pressure was 30 mW and 100 mTorr, respectively. In the calcination experiments, the samples were heated in a tube furnace purged with different gases at 500 °C and soaked for 1 h at a heating rate of 3−10 °C/min. To test the ultrahigh temperature stability, we transfer the sample to Si substrate and placed the film in the TGA chamber (TA Instruments SDT 2960 simultaneous DTA-TGA) and heated to 1100 °C for 1 h in Ar.

Templating 3D PDMS and PGMA Structures. For 3D PDMS, the PDMS prepolymer and curing agent (Sylgard 184 from Dow Corning) were mixed in a weight ratio of 10:1 and degassed for 2 h to re-

move air bubbles. The prepolymer mixture was then poured onto the POSS template at room temperature and waited for ~15 min to completely infiltrate the 3D porous template by capillary interaction. The composite film was cured at 65 °C for 2 h, followed by HF aqueous etching (~10 wt %) for ~50 min to remove the POSS template, resulting in an inverse 3D PDMS structure. During HF etching, a few droplets of dimethyl sulfoxide (DMSO) were added into the dilute HF solution (~10 mL) to enhance the wettability on the PDMS surface.

To prepare 3D PGMA, glycidyl methacrylate (GMA) monomers (Aldrich) were first mixed with 3 wt % of UV initiator (Darocur 1173, Ciba Specialty Chemicals) and prepolymerized by exposure to UV (97435 Oriel Flood Exposure Source) with a dosage ~1.0 J/cm^2. This viscous solution was then filled into the porous POSS template and covered by a transparent PDMS mold on top to reduce the exposure to O_2 in the air, which could inhibit the polymerization.[42] This sandwiched sample was then exposed to UV light again with a total dosage of ~14.4 mJ/cm^2 followed by HF etching to remove the POSS template. No organic solvent was added in HF solution during etching.

Characterization. The high-resolution SEM images were taken from FEI Strata DB235 focused ion beam (FIB) system at 5 kV. The lattice parameter in the (111) plane was measured from the top-view SEM images by average over two samples at three different locations by drawing lines in three different directions. The distance between the adjacent lattice planes in the [111] direction is measured from the focus-ion-beam-milled cross section. The samples were cut by FIB normal to the surface at an acceleration current of 1000 pA. The film shrinkage was estimated by comparing the measured lattice constants from SEM with the theoretically calculated values. Detailed calculation and reconstruction of the theoretical 3D structures were reported earlier.[29] The Fourier transform infrared (FT-IR) spectra were acquired using Nicolet 8700 equipped with Nicolet continuum infrared microscope. The samples were measured at a reflection mode with a MCT detector, and the aperture size used was about 80 μm × 80 μm. Energy-dispersive X-ray (EDX) analysis was performed on the 3D structures treated under different conditions using a high-resolution field emission scanning electron microscope (FESEM) JEOL 7500F coupled to an Oxford Si/Li detector and INCA software to study the overall chemical compositions of the 3D porous structures. The EDX spectra were acquired and collected at an acceleration voltage 13 keV after optimizing the experiment conditions. The refractive index of the POSS film was determined by an AutoEL-II Null ellipsometer (Rudolph Research, Flanders, NJ) at a fixed incident angle, 70°, with a helium−neon laser source (λ = 632.8 nm).

Optical Photographs. The photographs of 3D POSS and PDMS structures were taken by digital camera (NIKON, D300). The two pictures from 3D POSS before and after sintering were taken from two different samples at an illumination angle of ~45°. Both samples were from the same batch of 3D POSS fabricated under identical conditions. For the PDMS stretching experiments, the digital camera was located normal to the (111) plane of the 3D structure. The 3D PDMS film was clamped on two separated arms mounted on a custom-made ball bearing linear stage. The stretching strain was precisely controlled by the attached micrometer. Each frame was taken after the film was stretched to the desired strain level and held for ~30 s.

Acknowledgment. This research is supported by the Office of Naval Research (ONR), Grant No. N00014-05-0303, and Air Force of Scientific Research (AFOSR), Grant No. FA9550-06-1-0228. We thank Dr. Angang Dong and Prof. Christopher Murray for access to the FT-IR, and Dr. Yu Liu and Prof. Russell Composto for access to the ellipsometer. We acknowledge the Penn Regional Nanotechnology Facility (PRNF) for access to SEM and EDX analysis. We are grateful to Mr. Steve Szewczyk for setting up the tube-furnace for different heat treatment of our samples, and Mr. Felice Macera for digital photographing the optical images shown in Figure 6, Figure 9, and the video in the Supporting Information.

Supporting Information Available: EDX of 3D POSS structures treated under different conditions, and video demonstrating the color change of the 3D PDMS film under uniaxial stretching and release. This material is available free of charge *via* the Internet at http://pubs.acs.org.

REFERENCES AND NOTES

1. Joannopoulos, J. D.; Meade, R. D.; Winn, J. N. *Photonic Crystals*; Princeton University Press: Princeton, NJ, 1995.
2. Gorishnyy, T.; Ullal, C. K.; Maldovan, M.; Fytas, G.; Thomas, E. L. Hypersonic Phononic Crystals. *Phys. Rev. Lett.* **2005**, *94*, 4.
3. Jang, J. H.; Ullal, C. K.; Gorishnyy, T.; Tsukruk, V. V.; Thomas, E. L. Mechanically Tunable Three-Dimensional Elastomeric Network/Air Structures *via* Interference Lithography. *Nano Lett.* **2006**, *6*, 740–743.
4. Cumpston, B. H.; Ananthavel, S. P.; Barlow, S.; Dyer, D. L.; Ehrlich, J. E.; Erskine, L. L.; Heikal, A. A.; Kuebler, S. M.; Lee, I. Y. S.; McCord-Maughon, D.; *et al.* Two-Photon Polymerization Initiators for Three-Dimensional Optical Data Storage and Microfabrication. *Nature* **1999**, *398*, 51–54.
5. Jeon, S.; Malyarchuk, V.; White, J. O.; Rogers, J. A. Optically Fabricated Three Dimensional Nanofluidic Mixers for Microfluidic Devices. *Nano Lett.* **2005**, *5*, 1351–1356.
6. Therriault, D.; White, S. R.; Lewis, J. A. Chaotic Mixing in Three-Dimensional Microvascular Networks Fabricated by Direct-Write Assembly. *Nat. Mater.* **2003**, *2*, 265–271.
7. Lee, S. K.; Park, S. G.; Moon, J. H.; Yang, S. M. Holographic Fabrication of Photonic Nanostructures for Optofluidic Integration. *Lab Chip* **2008**, *8*, 388–391.
8. Holtz, J. H.; Asher, S. A. Polymerized Colloidal Crystal Hydrogel Films As Intelligent Chemical Sensing Materials. *Nature* **1997**, *389*, 829–832.
9. Lee, Y. J.; Braun, P. V. Tunable Inverse Opal Hydrogel pH Sensors. *Adv. Mater.* **2003**, *15*, 563–566.
10. Huang, J.; Hu, X. B.; Zhang, W. X.; Zhang, Y. H.; Li, G. T. pH and Ionic Strength Responsive Photonic Polymers Fabricated by Using Colloidal Crystal Templating. *Colloid Polym. Sci.* **2008**, *286*, 113–118.
11. Zhang, Y. J.; Wang, S. P.; Eghtedari, M.; Motamedi, M.; Kotov, N. A. Inverted-Colloidal-Crystal Hydrogel Matrices as Three-Dimensional Cell Scaffolds. *Adv. Funct. Mater.* **2005**, *15*, 725–731.
12. Jang, J. H.; Jhaveri, S. J.; Rasin, B.; Koh, C.; Ober, C. K.; Thomas, E. L. Three-Dimensionally-Patterned Submicrometer-Scale Hydrogel/Air Networks That Offer a New Platform for Biomedical Applications. *Nano Lett.* **2008**, *8*, 1456–1460.
13. Moon, J. H.; Ford, J.; Yang, S. Fabricating Three-Dimensional Polymeric Photonic Structures by Multi-Beam Interference Lithography. *Polym. Adv. Technol.* **2006**, *17*, 83–93.
14. Jang, J. H.; Ullal, C. K.; Maldovan, M.; Gorishnyy, T.; Kooi, S.; Koh, C. Y.; Thomas, E. L. 3D Micro- and Nanostructures *via* Interference Lithography. *Adv. Funct. Mater.* **2007**, *17*, 3027–3041.
15. Moon, J. H.; Yang, S. Chemical Aspects of Three-Dimensional Photonic Crystals. *Chem. Rev.* **2009**, DOI: 10.1021/cr900080v.
16. Tétreault, N.; von Freymann, G.; Deubel, M.; Hermatschweiler, M.; Pérez-Willard, F.; John, S.; Wegener, M.; Ozin, G. A. New Route to Three-Dimensional Photonic Bandgap Materials: Silicon Double Inversion of Polymer Templates. *Adv. Mater.* **2006**, *18*, 457–460.
17. Moon, J. H.; Yang, S.; Dong, W. T.; Perry, J. W.; Adibi, A.; Yang, S. M. Core−Shell Diamond-like Silicon Photonic Crystals from 3D Polymer Templates Created by Holographic Lithography. *Opt. Express* **2006**, *14*, 6297–6302.
18. Chabanov, A. A.; Jun, Y.; Norris, D. J. Avoiding Cracks in Self-Assembled Photonic Band-Gap Crystals. *Appl. Phys. Lett.* **2004**, *84*, 3573–3575.
19. Gratson, G. M.; Garcia-Santamaria, F.; Lousse, V.; Xu, M. J.; Fan, S. H.; Lewis, J. A.; Braun, P. V. Direct-Write Assembly of Three-Dimensional Photonic Crystals: Conversion of

Polymer Scaffolds to Silicon Hollow-Woodpile Structures. *Adv. Mater.* **2006**, *18*, 461–465.
20. Xu, Y.; Zhu, X.; Dan, Y.; Moon, J. H.; Chen, V. W.; Johnson, A. T.; Perry, J. W.; Yang, S. Electrodeposition of Three-Dimensional Titania Photonic Crystals from Holographically Patterned Microporous Polymer Templates. *Chem. Mater.* **2008**, *20*, 1816–1823.
21. Gonsalves, K. E.; Merhari, L.; Wu, H. P.; Hu, Y. Q. Organic−Inorganic Nanocomposites: Unique Resists for Nanolithography. *Adv. Mater.* **2001**, *13*, 703–714.
22. Tegou, E.; Bellas, V.; Gogolides, E.; Argitis, P.; Eon, D.; Cartry, G.; Cardinaud, C. Polyhedral Oligomeric Silsesquioxane (POSS) Based Resists: Material Design Challenges and Lithographic Evaluation at 157 nm. *Chem. Mater.* **2004**, *16*, 2567–2577.
23. Jun, Y.; Nagpal, P.; Norris, D. J. Thermally Stable Organic−Inorganic Hybrid Photoresists for Fabrication of Photonic Band Gap Structures with Direct Laser Writing. *Adv. Mater.* **2008**, *20*, 606.
24. George, M. C.; Nelson, E. C.; Rogers, J. A.; Braun, P. V. Direct Fabrication of 3D Periodic Inorganic Microstructures using Conformal Phase Masks. *Angew. Chem., Int. Ed.* **2009**, *48*, 144–148.
25. Moon, J. H.; Seo, J. S.; Xu, Y.; Yang, S. Direct Fabrication of 3D Silica-like Microstructures from Epoxy-Functionalized Polyhedral Oligomeric Silsesquioxane (POSS). *J. Mater. Chem.* **2009**, *19*, 4687–4691.
26. Matějeka, L.; Strachota, A.; Pleštil, J.; Whelan, P.; Steinhart, M.; Šlouf, M. Epoxy Networks Reinforced with Polyhedral Oligomeric Silsesquioxanes (POSS). Structure and Morphology. *Macromolecules* **2004**, *37*, 9449–9456.
27. Xu, M.; Gratson, G. M.; Duoss, E. B.; Shepherd, R. F.; Lewis, J. A. Biomimetic Silicification of 3D Polyamine-Rich Scaffolds Assembled by Direct Ink Writing. *Soft Matter* **2006**, *2*, 205–209.
28. Orilall, M. C.; Abrams, N. M.; Lee, J.; DiSalvo, F. J.; Wiesner, U. Highly Crystalline Inverse Opal Transition Metal Oxides *via* a Combined Assembly of Soft and Hard Chemistries. *J. Am. Chem. Soc.* **2008**, *130*, 8882–8883.
29. Zhu, X.; Xu, Y.; Yang, S. Distortion of 3D SU8 Photonic Structures Fabricated by Four-Beam Holographic Lithography with Umbrella Configuration. *Opt. Express* **2007**, *15*, 16546–16560.
30. Hayek, A.; Xu, Y.; Okada, T.; Barlow, S.; Zhu, X.; Moon, J. H.; Marder, S. R.; Yang, S. Poly(glycidyl methacrylate)s with Controlled Molecular Weights as Low-Shrinkage Resins for 3D Multibeam Interference Lithography. *J. Mater. Chem* **2008**, *18*, 3316–3318.
31. Bosworth, J. K.; Paik, M. Y.; Ruiz, R.; Schwartz, E. L.; Huang, J. Q.; Ko, A. W.; Smilgies, D. M.; Black, C. T.; Ober, C. K. Control of Self-Assembly of Lithographically Patternable Block Copolymer Films. *ACS Nano* **2008**, *2*, 1396–1402.
32. Wang, C. Y.; Shen, Z. X.; Zheng, J. Z. High-Temperature Properties of a Low Dielectric Constant Organic Spin-On Glass for Multilevel Interconnects. *Appl. Spectrosc.* **2001**, *55*, 1347–1351.
33. Liu, W. C.; Yang, C. C.; Chen, W. C.; Dai, B. T.; Tsai, M. S. The Structural Transformation and Properties of Spin-On Poly(silsesquioxane) Films by Thermal Curing. *J. Non-Cryst. Solids* **2002**, *311*, 233–240.
34. Socrates, G. *Infrared Characteristic Group Frequencies*, 2nd ed.; John Wiley & Sons Ltd.: West Sussex, England, 1994.
35. Guan, G.; Kusakabe, K.; Ozono, H.; Taneda, M.; Uehara, M.; Maeda, H. Fabrication and Structural Analysis of Three-Dimensionally Well-Ordered Arrangements of Silicon Oxycarbide Microparticles. *Chem. Eng. J.* **2008**, *135*, 232–237.
36. Leach, J. B.; Schmidt, C. E. Characterization of Protein Release from Photocrosslinkable Hyaluronic Acid−Polyethylene Glycol Hydrogel Tissue Engineering Scaffolds. *Biomaterials* **2005**, *26*, 125–135.
37. Norman, J. J.; Desai, T. A. Control of Cellular Organization in Three Dimensions Using a Microfabricated Polydimethylsiloxane−Collagen Composite Tissue Scaffold. *Tissue Eng.* **2005**, *11*, 378–386.
38. Lee, J. N.; Park, C.; Whitesides, G. M. Solvent Compatibility of Poly(dimethylsiloxane)-Based Microfluidic Devices. *Anal. Chem.* **2003**, *75*, 6544–6554.
39. Zhang, Y.; Matsumoto, E. A.; Peter, A.; Lin, P. C.; Kamien, R. D.; Yang, S. One-Step Nanoscale Assembly of Complex Structures *via* Harnessing of Elastic Instability. *Nano Lett.* **2008**, *8*, 1192–1196.
40. Lin, P. C.; Vajpayee, S.; Jagota, A.; Hui, C. Y.; Yang, S. Mechanically Tunable Dry Adhesive from Wrinkled Elastomers. *Soft Matter* **2008**, *4*, 1830–1835.
41. Fudouzi, H.; Xia, Y. N. Photonic Papers and Inks: Color Writing with Colorless Materials. *Adv. Mater.* **2003**, *15*, 892–896.
42. Chandra, D.; Taylor, J. A.; Yang, S. Replica Molding of High-Aspect-Ratio (Sub-)Micron Hydrogel Pillar Arrays and Their Stability in Air and Solvents. *Soft Matter* **2008**, *4*, 979–984.